

Molecular Selectivity of Brown Carbon Chromophores

J. Laskin,^{1,*} A. Laskin,^{2,*} S.A. Nizkorodov,³ P. Roach,¹ P. Eckert,² M.K. Gilles,⁴ B. Wang,² H.J. Lee,² Q. Hu¹

¹*Physical Sciences Division and ²Environmental Molecular Sciences Laboratory, Pacific Northwest National Laboratory, Richland, Washington 99352, USA;* ³*Department of Chemistry, University of California, Irvine, California 92697, USA;* ⁴*Chemical Sciences Division, Lawrence Berkeley National Laboratory, Berkeley, California 94720, USA*

*email: alexander.laskin@pnnl.gov, julia.laskin@pnnl.gov

*Supplemental file
8 pages, 2 figures, 2 tables*

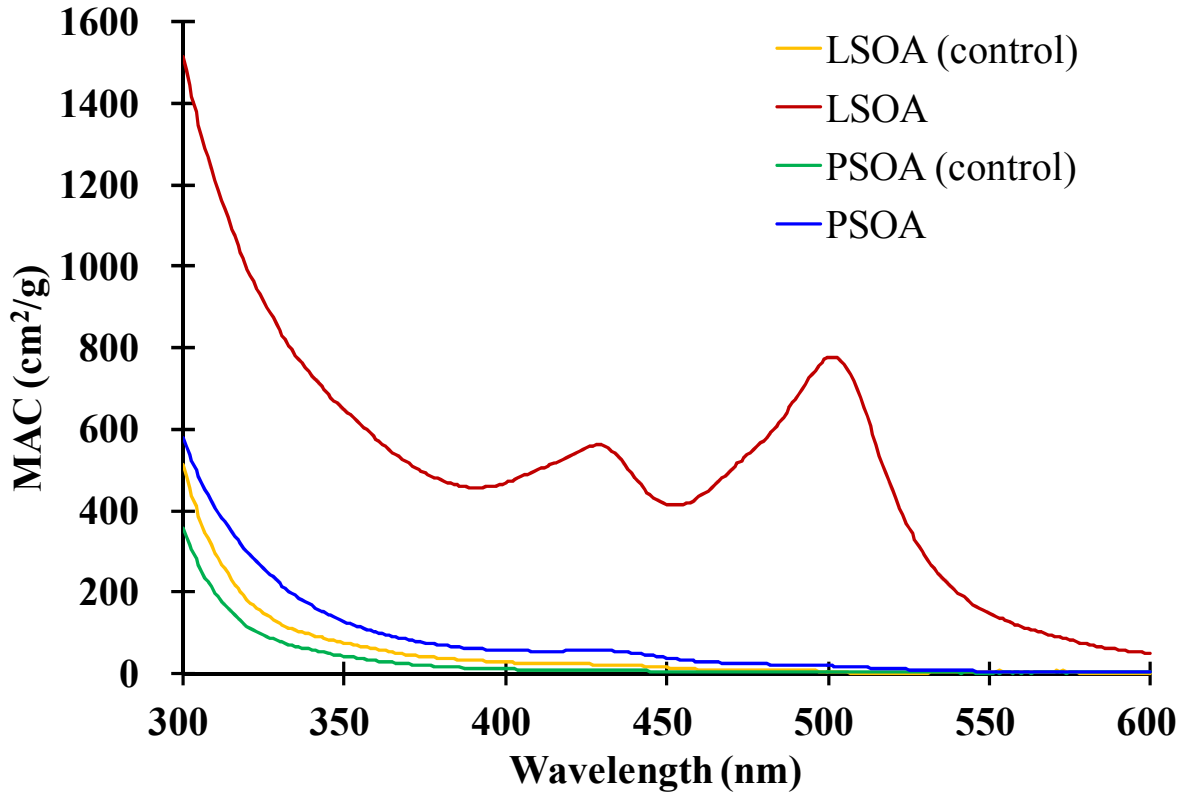


Figure S1. UV-Vis spectra of LSOA and PSOA before and after aging with NH_3 . The figure is compiled using previously published data of *Lee et al.* (2013).^a The control samples of LSOA and PSOA were exposed to humidified air free of NH_3 using the same setup as in the aging experiment. For UV-Vis measurements, the aged and control samples of LSOA and PSOA with measured mass loadings were extracted in deionized water. Efficiency of water extraction for these samples has been evaluated as better than 90% (*Updyke et al*, 2012)^b. Browning of LSOA and PSOA samples was quantified as a difference between mass absorption coefficients (MAC) integrated over 300-700 nm spectral range for NH_3 -aged and control samples $\langle \Delta \text{MAC}_{300-700} \rangle$, respectively. The wavelength-dependent values of $\text{MAC}(\lambda)$ ($\text{cm}^2 \text{ g}^{-1}$) were inferred from the UV-Vis absorption measurements for SOA extracts using equation E1 (*Chen and Bond*, 2010)^c

$$\text{MAC}(\lambda) = \frac{A_{10}(\lambda) \times \ln(10)}{b \times C_{\text{mass}}} \quad (\text{E1})$$

where $A_{10}(\lambda)$ is the base-10 absorbance of the sample extract with mass concentration C_{mass} (g cm^{-3}) measured over optical pathlength b (cm). The wavelength-averaged values of $\langle \text{MAC}_{300-700} \rangle$ were obtained using equation E2 (*Updyke et al*, 2012)^b

$$\langle \text{MAC}_{300-700} \rangle = \frac{1}{(700 - 300) \text{nm}} \times \int_{300 \text{nm}}^{700 \text{nm}} \text{MAC}(\lambda) d\lambda \quad (\text{E2})$$

The browning extent is then reported as $\langle \Delta MAC_{300-700} \rangle = \langle \Delta MAC_{300-700} \rangle_{aged} - \langle \Delta MAC_{300-700} \rangle_{control}$.

^aLee, H. J.; Laskin, A.; Laskin, J.; Nizkorodov, S. A., Excitation-Emission Spectra and Fluorescence Quantum Yields for Fresh and Aged Biogenic Secondary Organic Aerosols. *Environmental Science & Technology* 2013, 47, (11), 5763-5770.

^bUpdyke, K. M.; Nguyen, T. B.; Nizkorodov, S. A., Formation of brown carbon via reactions of ammonia with secondary organic aerosols from biogenic and anthropogenic precursors. *Atmospheric Environment* 2012, 63, 22-31.

^cChen, Y., Bond, T.C., 2010. Light absorption by organic carbon from wood combustion. *Atmos. Chem. Phys.* 10 (4), 1773e1787.

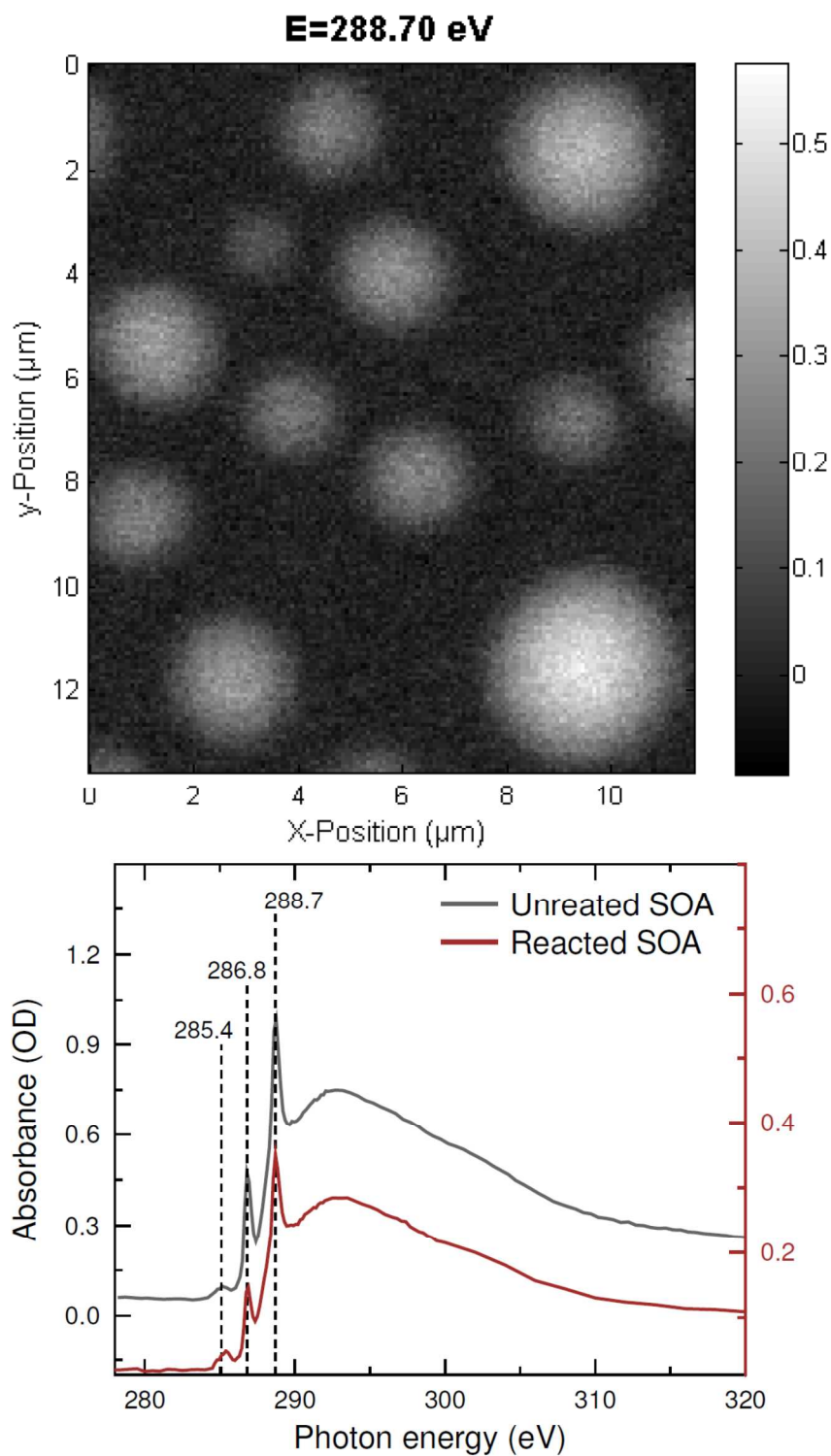


Figure S2. Upper panel: STXM images of LSOA particles taken at fixed 288.7 eV energy. Particles shown in this sample were collected on the 6th stage (aerodynamic size range: 0.56-1.0 μm) of MOUDI. Their substantially larger 2D- projection areas are a result of particle flattening upon the impaction (Bateman et al, 2009; O'Brien et al, 2014)^b

Lower panel: Comparison of representative Carbon-edge NEXAFS spectra acquired over the areas of individual LSOA particles before and after aging with ammonia. The spectra show nearly no detectable changes in the LSOA composition after aging. A slight blue shift of the spectral feature at 285.4 eV (C 1s→π* transition in C=C) (*Moffet et al, 2010*)^c can be possibly inferred from comparison of the spectra, which would be consistent with formation of the Schiff base products and characteristic C 1s→π* transitions in C=N bonds at higher energy of 285.9 eV (*Shard et al, 2004*)^d. However, the low intensity of this peak and insufficient energy resolution make even this change ambiguous.

^bBateman, A. P.; Nizkorodov, S. A.; Laskin, J.; Laskin, A., Time-resolved molecular characterization of limonene/ozone aerosol using high-resolution electrospray ionization mass spectrometry. *Physical Chemistry Chemical Physics*, 2009, 11, (36), 7931-7942; R.E. O'Brien, A. Neu, S.A. Epstein, A.C. MacMillan, B. Wang, S.T. Kelly, S.A. Nizkorodov, A. Laskin, R.C. Moffet, M.K. Gilles. Phase State and Physical Properties of Ambient and Laboratory Generated Secondary Organic Aerosol. *Geophysical Research Letters*, 2014, 41, 4347–4353. doi:10.1002/2014GL060219.

^cMoffet, R. C.; Tivanski, A. V.; Gilles, M. K., Scanning X-ray Transmission Microscopy: Applications in Atmospheric Aerosol Research. In *Fundamentals and Applications in Aerosol Spectroscopy*, Signorell, R.; Reid, J. P., Eds. Taylor and Francis Books, Inc: 2010; pp 419-462.

^dShard, A. G.; Whittle, J. D.; Beck, A. J.; Brookes, P. N.; Bullett, N. A.; Talib, R. A.; Mistry, A.; Barton, D.; McArthur, S. L., A NEXAFS examination of unsaturation in plasma polymers of allylamine and propylamine. *Journal of Physical Chemistry B* 2004, 108, (33), 12472-12480.

Table S1. Normalized abundances of $[M+H]^+$ and $[M+Na]^+$ peaks corresponding to the major ozonolysis products of limonene and α -pinene in nano-DESI/HRMS spectra of fresh LSOA and PSOA samples.

Neutral Mass, Da	Formula	LSOA $[M+Na]^+$	LSOA $[M+H]^+$	PSOA $[M+Na]^+$	PSOA $[M+H]^+$	Literature Assignments for Limonene ^a	Literature Assignments for α -pinene ^b
140.0837	$C_8H_{12}O_2$		0.5		7.3		2,2-dimethyl-cyclobutyl-1,3-dicarboxaldehyde
154.0994	$C_9H_{14}O_2$		1.8	0.9	5.7		Norpinaldehyde
156.0786	$C_8H_{12}O_3$				8.6		Norpinalic acid
168.1150	$C_{10}H_{16}O_2$	0.5			28.8	Limonaldehyde	Pinonaldehyde
170.0943	$C_9H_{14}O_3$	2.1	0.6	2.9	24.2	Keto-lemonaldehyde or Limonic acid	Norpinonic acid
172.0736	$C_8H_{12}O_4$	2.4		0.3	4.2	Keto-limonalic acid	Norpinic acid
182.0943	$C_{10}H_{14}O_3$	0.6	3.9	0.1	20.8		Hydroxy pinonaldehyde
184.1099	$C_{10}H_{16}O_3$	26.9	2.6	7.9	38.5	Limononic acid	Pinonic acid
186.0892	$C_9H_{14}O_4$	100.0	2.9	0.8	7.5	Limonic acid	Pinic acid
198.0892	$C_{10}H_{14}O_4$	0.7	1.9	0.3	10.1		
200.1049	$C_{10}H_{16}O_4$	56.4	3.4	2.1		Hydroxy-limononic acid	Hydroxy pinonic acid ^c
202.0841	$C_9H_{14}O_5$	10.1		1.7	1.8		

^a Walser, M. L.; Desyaterik, Y.; Laskin, J.; Laskin, A.; Nizkorodov, S. A., High-resolution mass spectrometric analysis of secondary organic aerosol produced by ozonation of limonene. *Physical Chemistry Chemical Physics* 2008, 10, (7), 1009-1022.

^b Yu, J.; Cocker, D.R.; Griffin, R.J.; Flagan, R.C.; Seinfeld, J.H., Gas-Phase Ozone Oxidation of Monoterpenes: Gaseous and Particulate Products. *Journal of Atmospheric Chemistry* 1999, 34, 207–258.

^c Fache, F.; Piva, O.; Mirabel, P., First synthesis of hydroxy-pinonaldehyde and hydroxy-pinonic acid, monoterpene degradation products present in atmosphere. *Tetrahedron Letters*, 2002, 43, 2511–2513.

Table S2. Neutral masses (Da), normalized abundances (%), double bond equivalents (DBE), and formula assignments of the most abundant species identified in nano-DESI/HRMS spectra of the fresh and aged LSOA and PSOA. The CHO, CHON1 and CHON2 types of the compounds are indicated at the beginning of each subsection of the table.

Neutral Mass	Normalized Abundance				DBE	Neutral Formula
	Fresh LSOA	Fresh PSOA	Aged LSOA	Aged PSOA		
CHO						
148.0888	0	17	5	10	5	C10H12O
150.1045	0	52	5	54	4	C10H14O
152.0837	1	12	29	15	4	C9H12O2
154.0994	2	6	27	5	3	C9H14O2
164.0837	3	9	21	6	5	C10H12O2
166.0994	8	100	100	100	4	C10H14O2
168.0786	8	13	32	15	4	C9H12O3
168.1150	0	29	9	28	3	C10H16O2
170.0943	1	24	9	43	3	C9H14O3
182.0943	4	21	34	20	4	C10H14O3
184.1099	30	46	33	70	3	C10H16O3
186.0892	100	9	12	14	3	C9H14O4
198.0892	2	10	12	8	4	C10H14O4
200.1049	56	2	0	2	3	C10H16O4
320.1988	0	12	3	21	6	C19H28O4
336.1937	1	13	6	26	6	C19H28O5
338.2093	7	10	10	9	5	C19H30O5
340.1886	19	6	12	6	5	C18H28O6
342.1679	17	1	5	2	5	C17H26O7
342.2042	11	0	13	4	4	C18H30O6
344.1835	15	2	8	3	4	C17H28O7
352.1886	1	12	8	16	6	C19H28O6
352.2250	4	47	0	17	5	C20H32O5
354.2042	24	24	22	20	5	C19H30O6
356.1835	30	5	13	6	5	C18H28O7
356.2199	9	3	17	3	4	C19H32O6
358.1992	18	0	15	4	4	C18H30O7
366.2042	1	13	7	9	6	C20H30O6
368.1835	19	3	5	3	6	C19H28O7
368.2199	11	25	0	13	5	C20H32O6
370.1992	39	24	28	14	5	C19H30O7
372.1784	27	2	0	3	5	C18H28O8
372.2148	15	4	0	6	4	C19H32O7
374.1941	13	2	9	3	4	C18H30O8

382.1992	9	10	4	2	6	C20H30O7
384.2148	35	16	0	8	5	C20H32O7
386.1941	52	8	24	8	5	C19H30O8
386.2305	12	2	21	1	4	C20H34O7
400.2097	32	13	19	7	5	C20H32O8
402.1890	23	4	0	4	5	C19H30O9
416.2046	16	5	8	2	5	C20H32O9

CHON1

165.0790	0	0	10	0	5	C9H11NO2
167.0946	0	0	13	1	4	C9H13NO2
281.2719	13	1	0	1	2	C18H35NO
315.3137	41	21	0	11	0	C19H41NO2
335.2097	0	0	7	27	6	C19H29NO4
337.1889	0	0	0	15	6	C18H27NO5
349.2253	0	1	13	25	6	C20H31NO4
351.2046	0	0	17	55	6	C19H29NO5
355.2359	0	7	4	14	4	C19H33NO5
365.2202	0	1	0	18	6	C20H31NO5
367.1995	0	0	0	26	6	C19H29NO6
369.2515	0	68	6	44	4	C20H35NO5
371.2308	3	26	0	38	4	C19H33NO6
373.2101	4	4	6	9	4	C18H31NO7
383.2308	0	10	2	10	5	C20H33NO6
385.2464	1	21	6	22	4	C20H35NO6
387.2257	6	26	10	29	4	C19H33NO7
389.2050	5	2	5	4	4	C18H31NO8
389.2414	2	3	10	8	3	C19H35NO7
399.2257	1	9	0	6	5	C20H33NO7
401.2414	5	16	9	13	4	C20H35NO7
403.2206	8	7	9	12	4	C19H33NO8
403.2570	2	1	6	2	3	C20H37NO7
405.2363	2	2	9	4	3	C19H35NO8

CHON2

312.1838	0	0	2	0	9	C19H24N2O2
438.2519	0	0	5	0	11	C26H34N2O4
440.2311	0	0	3	0	11	C25H32N2O5
450.2519	0	0	2	0	12	C27H34N2O4
452.2675	0	0	23	0	11	C27H36N2O4
454.2468	0	0	6	0	11	C26H34N2O5
466.2832	0	0	12	0	11	C28H38N2O4
468.2624	0	0	4	0	11	C27H36N2O5
482.2781	0	0	2	0	11	C28H38N2O5